AJNR

Cerebral Perfusion Alterations during the Acute Phase of Experimental Generalized Status Epilepticus: Prediction of Survival By Using Perfusion-Weighted MR Imaging and Histopathology

T. Engelhorn, A. Doerfler, J. Weise, M. Baehr, M. Forsting and A. Hufnagel

AJNR Am J Neuroradiol 2005, 26 (6) 1563-1570
http://www.ajnr.org/content/26/6/1563

Cerebral Perfusion Alterations during the Acute Phase of Experimental Generalized Status Epilepticus: Prediction of Survival By Using Perfusion-Weighted MR Imaging and Histopathology

T. Engelhorn, A. Doerfler, J. Weise, M. Baehr, M. Forsting, and A. Hufnagel

BACKGROUND AND PURPOSE: **Persistent generalized status epilepticus (SE) is associated with alterations of cerebral perfusion (CP). Because perfusion-weighted MR imaging (PWI) allows noninvasive CP-determination, the aim of this study was to investigate CP alterations during acute experimental SE correlated with SE-induced neuronal cell loss.**

METHODS: **The rat pilocarpine model was used to induce SE. Multilocal PWI was performed before (baseline) and 3, 15, 30, 60, and 120 minutes after onset of SE. Bolus-peak ratio (BPR) was calculated for the retrosplenial and piriform cortex, hippocampus, amygdala, and thalamus and compared with baseline. Neuronal cell loss was quantified at different time points after induction of SE by cresyle violet staining.**

RESULTS: **Immediately after SE onset (3 minutes), BPR temporarily increased to 102%–130% in all regions, with a maximum in the amygdala (129 ± 16%) and hippocampus (130 ± 21%). At 15, 30, and 60 minutes, BPR decreased continuously to 57%–76%. BPR values <55% in the parietal and/or temporal cortex resulted in death. In surviving animals, BPR recovered to 66%–79% and there was a good correlation between neuronal cell loss in specific brain regions at 2 weeks after SE onset and maximal decrease in BPR ($r > 0.73$).**

CONCLUSION: **PWI demonstrated a transient cerebral hyperperfusion immediately after SE onset, followed by a significant continuous decline to different perfusion levels. In our experimental setting, a decline of cortical BPR below 55% of baseline seems to be a prognostic threshold value associated with subsequent death. In surviving animals, there is good correlation between the maximal decrease in BPR in the acute phase of SE and late neuronal cell loss.**

Status epilepticus (SE) is a condition that may result in significant morbidity as well as mortality (1). Potential long-term sequelae include cognitive decline and enhancement of further seizure activity (2–5). Alterations in local cerebral perfusion, as well as the rapid development of cytotoxic and vasogenic edema in the early phase, may represent functional changes, but also have been claimed to lead to subsequent neuronal loss.

Neuroimaging techniques are useful aids in the diagnosis of SE. Positron-emission tomography identifies seizure foci as ictal increases in glucose metabolism and cerebral blood flow and interictal decreases in these measures (6, 7). Similar changes in cerebral blood flow are detectable by single-photon emission CT (SPECT; 8, 9).

Because noninvasive MR imaging is part of the standard diagnostic workup of patients with seizure disorders to detect brain lesions that are visible on T1- and T2-weighted images (3, 4), it would be advantageous to have a physiologic MR imaging method to predict the severity of SE (ie, the extend of loss of neurons) in the very early phase of SE.

Local hyper- and hypoperfusion of brain parenchyma during epileptic activity have been demonstrated with dynamic perfusion-weighted MR imaging (PWI) in a small number of case reports (10–12), a technique extensively used to detect and monitor the evolution of ischemic brain damage in experimental

Received August 17, 2004; accepted November 8.

From the Departments of Neuroradiology (T.E., A.D., M.F.) and Neurology (A.H.), University of Essen, Essen, Germany; and the Department of Neurology (J.W., M.B.), University of Goettingen, Goettingen, Germany.

Address correspondence to Tobias Engelhorn, MD, Department of Neuroradiology, Essen University School of Medicine, Hufelandstrasse 55, D-45122 Essen, Germany.

and clinical settings (13, 14). Systematic experimental examination of cerebral perfusion alterations during the acute phase of seizure-induced damage by using PWI, however, is lacking. Furthermore, no correlative studies comparing PWI with the analysis of neuronal cell loss have been reported. To the best of our knowledge, this is the first study which describes PWI changes that occur during the acute phase of SE and subsequent histologic changes.

We used the rat pilocarpine model, a well-established animal model, leading to SE in the acute phase and subsequently to the development of temporal lobe epilepsy in the postacute phase. Behavioral aspects, electrophysiology, and gross histopathology in this model are well characterized (15–18). We hypothesize that changes in cerebral blood flow measured by PWI correlate with seizure-induced neuronal damage in different brain areas as determined by histologic analysis. Clinically, the possibility to identify subtle histopathologic alterations with noninvasive MR imaging in the early phase of an ictal event would be of significant therapeutic relevance.

Methods

Animals and Seizure Assessment

For all experiments male Sprague-Dawley rats (280–320 g) were used. Animals were allowed free access to food. The study was approved by the institutional review board of the medical facility, district of Düsseldorf, Germany.

For preparation, all animals were shortly anesthetized initially with 2% isoflurane to catheterize the femoral artery and vein to monitor blood pressure and blood gases and to administer contrast agent for PWI. Anesthesia was maintained with fentanyl (0.1 mg/kg per hour intravenously) during MR imaging until SE onset. Body temperature was maintained at 37 ± 0.5°C with a feedback-regulated heating pad. Heart rate and SaO_2 were continuously monitored by a pulse oximeter.

Before induction of SE, all animals were positioned in the MR scanner to acquire baseline scans, firmly held by an especially designed MR-compatible head holder, allowing reliable fixation to avoid seizure-related movements.

After baseline scans, SE was induced by administration of freshly dissolved pilocarpine hydrochloride (360 mg/kg 000000 [intraperitoneal]), a cholinerge antagonist, without removing animals from the MR scanner. The injection protocols were similar to those described elsewhere (19–21). Peripheral cholinergic effects were minimized by i.p. injection of 1 mg/kg scopolamine methyl nitrate at 30 minutes before pilocarpine administration (15, 22). Saline-injected animals ($n = 3$) served as controls.

After injection of pilocarpine hydrochloride, the animal's behavior was monitored by a camera system. Only animals that demonstrated onset of continuous generalized seizures were included in the present study. These animals were then studied with PWI performed at 3, 15, 30, 60, and 120 minutes after onset of pilocarpine-induced seizures. After MR examination, animals could recover and were allowed free access to food.

MR Imaging

MR baseline scans (PWI and T1-weighted imaging) were performed on each rat before the injection of pilocarpine. Only animals that demonstrated a normal brain anatomy were included. Additional control scans were performed in three saline-treated animals to confirm that no PWI changes had occurred because of animal handling and injections. Imaging was performed on a 1.5-T MR unit (Sonata, Siemens, Erlangen, Germany) with a 50-mm-diameter, small field-of-view orbita surface coil. Scout images were obtained in the coronal, axial, and transverse planes to position the sections accurately. Five coronal sections, each with 2-mm thickness and 0.2-mm separation (interslice gap) were positioned on the transverse scout images at the level of the hippocampal formation and piriform cortex. PWI was performed by using a spin-echo, echo planar imaging (EPI) sequence to follow the passage of a bolus application of 0.3 mmol/kg gadolinium diethylene triamine pentaacetic acid (Magnevist, Schering, Berlin), given by an automatic injector with a flow-rate of 0.3 mL/min (23). The EPI images were acquired with a 128 × 128 matrix; 43-mm field of view; 1-second repetition time; 88-millisecond echo time; and one average. Forty sets of five sections were acquired continuously for 40 seconds. The T1-weighted images were acquired with a 128 × 128 matrix; 50-mm field of view; 500-millisecond repetition time; 14-millisecond echo time; two averages; eight coronal sections; and 1.5-mm section thickness.

Image Analysis

Imaging analysis was performed for each rat on a single section located immediately anterior to the section where the hippocampus can be seen curling inferiorly as recently described in detail by Wall et al (24). The position of the section corresponded approximately to bregma −3.6 mm and maximized the cross-sectional area of each region of interest (25). Siemens built-in image-processing software (Siemens, Erlangen, Germany) was used to outline and analyze the regions of interest that were confirmed by a second investigator. The bilateral regions of interest included the amygdala and associated nuclei, the retrosplenial parietal cortex (including motor and somatosensory cortex), the retrosplenial temporal cortex, the piriform cortex (including parts of the entorhinal and perirhinal cortex), the thalamus, and the hippocampus (CA 1–3).

A 2-pixel width separated the ventral hippocampus and retrosplenial parietal and temporal cortex. A line drawn across the bottom of both hippocampi that extended across the cortex demarcated the inferior border of the temporal cortex (outlined as a 4 × 4 pixel square). The piriform and amygdala regions of interest abutted each other and extended the same distance superiorly and inferiorly. Medially, four pixels separated the thalamus from the amygdala to minimize signal intensity contribution from the lateral ventricle. A 5 × 5 pixel square was centered within the thalamus. All regions of interest are outlined in Fig 1.

In all regions of interest, as a semiquantitative measure of cerebral perfusion, the bolus-peak ratio (BPR) in the bolus-tracking curves was calculated at 3, 15, 30, 60, and 120 minutes after onset of pilocarpine-induced seizures and was normalized relative to the corresponding regions under baseline conditions (26). Thereby, BPR in the regions of interest after onset of SE ($t = x$) as compared with baseline conditions ($t = 0$) are given by:

$$\mathrm{BPR} = [(\text{maximal signal intensity loss region of interest}_{t=x})/(\text{maximal signal intensity loss region of interest}_{t=0})] \times 100.$$

Because the signal intensity loss in the region of interest must be normalized with respect to the corresponding region of interest at baseline conditions that presumably has normal perfusion, a BPR of 100% would imply normal perfusion, and 0% would indicate no perfusion.

Tissue Preparation and Analysis of Neuronal Cell Loss

The animals were allocated to the different time points of histology by using a computer randomization scheme (Table 1). After i.p. injection with chloralhydrate (7% in phosphate-buff-

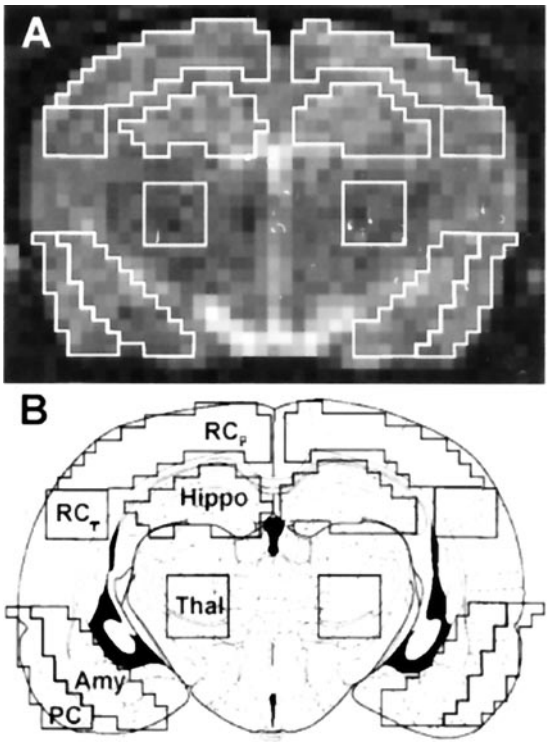

FIG 1. Regions of interest used for quantitative analysis. *A,* Representative MR image on which regions of interest are outlined. *B,* Schematic drawing of a rat brain at similar level with identical regions of interest superimposed. regions of interest were defined as: retrosplenial parietal and temporal cortex (RC_P and RC_T), piriform cortex (PC), hippocampus (Hippo), thalamus (Thal), and amygdala (Amy).

ered saline, 420 mg/kg body weight), they were transcardialy perfused with paraformaldehyde (4% in 0.12 mol/L Millonig phosphate buffer) at 30 minutes (during SE) and 2 hours (during SE, after completion of imaging) as well as 1, 7, and 14 days after SE induction ($n = 2$ for all time points). For early histology, we chose 0.5 hours after SE induction, because we calculated the maximal decline in BPR at this time point (prestudies) and 2 hours as end point measurement after the MR monitoring. Three untreated animals served as controls.

Brains were removed and shock-frozen in liquid nitrogen. Cryosections were prepared and stained with cresyle violet solution (Nissl-staining) to identify neuronal cells. Neuronal cell counts were performed in the hippocampus (CA1–3), amygdala, piriform/temporal/parietal cortex, and the thalamus in six sections of each animal per region and time point. Depending on the region and its neuronal attenuation, areas analyzed varied between 0.1 and 0.4 mm^2. For better comparison of SE-induced neuronal cell loss in different brain regions, the number of neurons, after counting absolute numbers, were given as percentage of the corresponding control value.

Statistical Analysis of the Data

For statistical analysis of all results, commercial software (StatView, Brain Power, Calabasas, CA) was used. Left and right comparison of bilateral regions of interest compared with baseline was performed for each animal by use of one-way analysis of variance. A two-tailed Student's t test was performed to compare baseline/control values with the experimental values at each time point after the onset of seizures and for saline injected/untreated controls. Linear regression analyses between maximal and minimal flow indices and cell counts were performed. A probability value of $P < .05$ was considered to be significant—denoted with an asterisk (*) in the tables and figures. The means and standard deviations (SDs) are presented for the various groups.

Results

All animals revealed normal brain anatomy on the T1-weighted MR images before pilocarpine injection. Injection of pilocarpine in 32 animals resulted in 20 animals (62.5%) developing generalized status epilepticus for inclusion in the present study. Saline controls were performed in three animals, and no behavioral abnormalities were observed after injection. Behavioral seizures often began 15–40 minutes after pilocarpine injection and were similar to previous reports (15, 16). Table 1 demonstrates number of animals used at each of the imaging time points and for histology.

Throughout the surgical preparation, the average body temperature for all animals was 36.9 ± 0.5°C (mean ± SD). Arterial blood gases ($pO_2 = 103 \pm 19$ mmHg; $pCO_2 = 38 \pm 6$ mmHg; pH = 7.37 ± 0.04) and hematocrit (40.6 ± 2.8%) remained stable. Two hours after the onset of seizures, the average body temperature was significantly increased to 37.8 ± 0.7°C, whereas arterial blood gases did not change significantly.

Changes in Cerebral Blood Flow after SE

In controls and pilocarpine treated animals, there was no significant difference between identical regions of interest of the left and right hemisphere at any time point of MR examination ($P > .28$). Therefore, BPRs of identical regions of interest were averaged.

No significant changes in BPR were observed in control animals at 3, 15, 30, 60, and 120 minutes after saline injection, with 102 ± 5%, 100 ± 4%, 101 ± 5%, 102 ± 4% and 102 ± 5%, respectively, compared with baseline ($P > .42$).

Averaged BPRs of pilocarpine treated animals at baseline conditions and at 3, 15, 30, 60, and 120 minutes after the onset of seizures for the examined regions of interest are presented in Figs 2–7.

At 3 minutes after onset of seizures, BPR was significantly increased in the parietal, temporal and piriform cortex, the amygdala, and hippocampus, with 130 ± 34%, 112 ± 10%, 114 ± 12%, 129 ± 16%, and 130 ± 21%, respectively, compared with baseline ($P < .05$). At this time point, no significant change in BPR was seen in the thalamus, with 102 ± 16% compared with baseline ($P = .77$).

At 15, 30, 60, and 120 minutes after the onset of seizures, all animals revealed a significant decrease in BPR compared with baseline ($P < .05$). The maximal decrease in BPR in the parietal, temporal and piriform cortex and thalamus was seen at 30 minutes after the onset of seizures, with 70 ± 8%, 61 ± 17%, 76 ± 15%, and 72 ± 12%, respectively, compared with baseline. The maximal decrease in BPR in the amygdala and the hippocampus was seen at 60 minutes after the onset of seizures, with 62 ± 11% and 65 ± 9%, respectively, compared with baseline.

Six of 20 animals did not survive the 2-hour period

TABLE 1: Number of animals undergoing PWI at different time points after pilocarpine-induced SE (PWI-SE) or saline injection (PWI-control) and analysis of neuronal cell death (histology) at different time points after SE induction (untreated = control)

	Untreated	3 min	15 min	0.5 h	1 h	2 h	1 d	1 wk	2 wk
PWI-SE		20	20	20	15	12	–	–	–
PWI-control		3	3	3	3	3	–	–	–
Histology	3			2		2	2	2	2

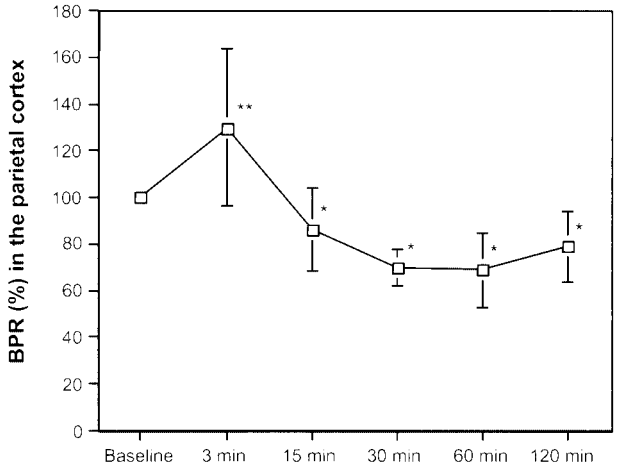

FIG 2. Averaged BPRs in the retrosplenial parietal cortex of pilocarpine-treated animals at baseline conditions and at 3, 15, 30, 60, and 120 minutes after pilocarpin-induced SE, respectively. An asterisk denotes significant decease compared with baseline conditions. A double asterisk denotes significant increase compared with baseline conditions.

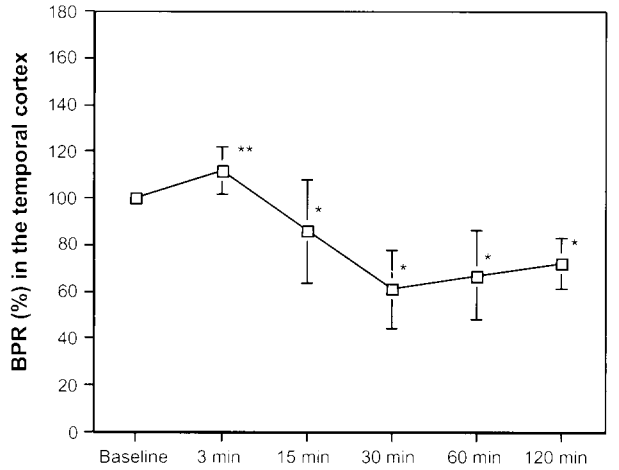

FIG 3. Averaged BPRs in the retrosplenial temporal cortex of pilocarpine -treated animals at baseline conditions and at 3, 15, 30, 60, and 120 minutes after pilocarpin-induced SE, respectively. An asterisk denotes significant decease compared with baseline conditions. A double asterisk denotes significant increase compared with baseline conditions.

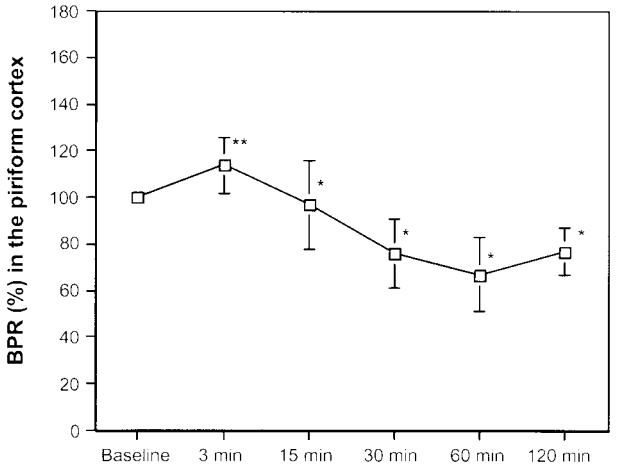

FIG 4. Averaged BPRs in the piriform cortex of pilocarpine-treated animals at baseline conditions and at 3, 15, 30, 60, and 120 minutes after pilocarpin-induced SE, respectively. An asterisk denotes significant decease compared with baseline conditions. A double asterisk denotes significant increase compared with baseline conditions.

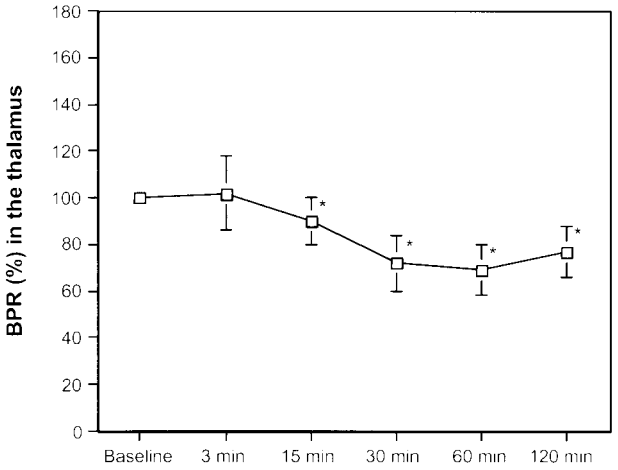

FIG 5. Averaged BPRs in the thalamus of pilocarpine-treated animals at baseline conditions and at 3, 15, 30, 60, and 120 minutes after pilocarpin-induced SE, respectively. An asterisk denotes significant decease compared with baseline conditions.

of seizures. The 2-hour mortality rate was 30%. All of these animals died 30–60 minutes after the onset of seizures. In these animals, BPR in the parietal and/or temporal cortex immediately before death decreased to <55% compared with baseline. Compared with surviving animals, this decrease in BPR was significantly higher. In contrast, BPR in the piriform cortex, thalamus, amygdala, and hippocampus immediately before death was not significantly different than that of surviving animals. In surviving animals, BPR recovered to 66%–79% compared with baseline at 2 hours after the onset of seizures.

Neuronal Cell Loss after SE

Cresyl violet staining of brain sections from controls revealed normal neuronal morphology in all of the brain regions examined. There was no statistically significant neuronal cell loss in all brain regions analyzed at 0.5 and

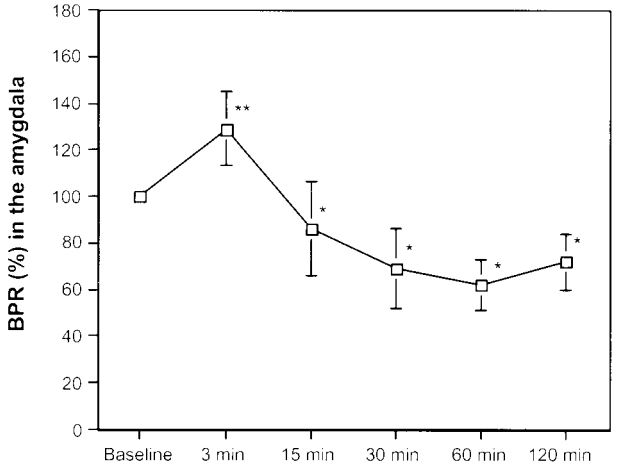

FIG 6. Averaged BPRs in the amygdala of pilocarpine-treated animals at baseline conditions and at 3, 15, 30, 60, and 120 minutes after pilocarpin-induced SE, respectively. An asterisk denotes significant decease compared with baseline conditions. A double asterisk denotes significant increase compared with baseline conditions.

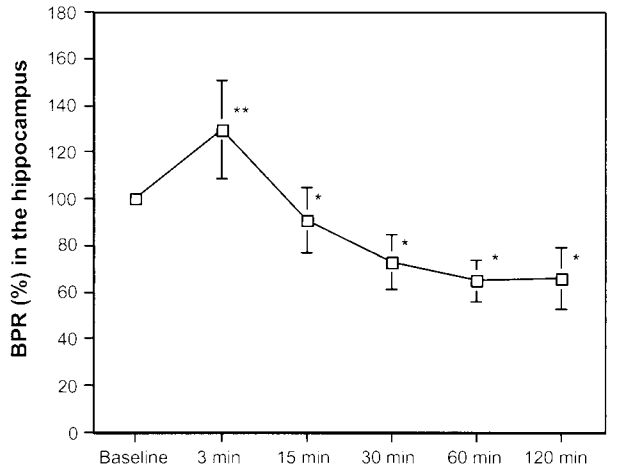

FIG 7. Averaged BPRs in the hippocampus of pilocarpine-treated animals at baseline conditions and at 3, 15, 30, 60, and 120 minutes after pilocarpin-induced SE, respectively. An asterisk denotes significant decease compared with baseline conditions. A double asterisk denotes significant increase compared with baseline conditions.

2 hours after SE induction compared with controls ($P < .05$); however, at 1 day as well as 1and 2 weeks after the onset of seizures, we observed a significant decline in the number of neurons compared with controls in all of the examined brain regions. Maximal neuronal cell loss in all examined brain regions was seen at 2 weeks after SE induction, and it was most pronounced in the piriform cortex (surviving neurons, 32 ± 4%) and the amygdala (surviving neurons, 38 ± 5%). The different extent of neuronal cell death in all brain regions examined at 0.5, 2, and 24 hours and at 1 and 2 weeks after SE induction is presented in Table 2.

Correlation of Blood Flow Alterations and Neuronal Cell Loss

There was a good correlation between the maximal decrease in BPR between 30 and 60 minutes after onset of seizures and the maximal neuronal cell loss in the examined brain regions in the two animals undergoing MR examination and histology at 1 day after onset of seizures ($r > 0.63$), at 1 week after onset of seizures ($r > 0.66$) and at 2 weeks after onset of seizures ($r > 0.73$). At 0.5 and 2 hours after onset of seizures, there was only poor correlation ($r < 0.31$). In addition, there was poor correlation between the maximal increase in BPR and the maximal neuronal cell loss ($r < 0.54$).

Discussion

To the best of our knowledge, the present experimental study is the first investigation of the effects of generalized status epilepticus on MR measured cerebral blood flow in different brain regions in the very early phase of SE (3 minutes to 2 hours after the onset of seizures) in the rat pilocarpine model. In addition, effects on neuronal cell loss at 0.5 hours to 2 weeks after the onset of seizures were assessed histologically and correlated with the MR-derived cerebral blood flow alterations.

The novel findings of the present study are (1) a significant increase in cerebral blood flow immediately after the onset of seizures in the retrosplenial and piriform cortex, the amygdala, and the hippocampus (blood flow in the thalamus remained stable) followed by (2) a significant continuous decrease in blood flow to 57%–76% of baseline in all examined brain regions 0.5–1 hour after the onset of seizures. Thereby, (3) a decline of retrosplenial cortical blood flow below 55% of baseline seems to be a prognostic threshold value associated with subsequent death of the animal. In addition, (4) the extent of decreased blood flow in the early phase of seizures gives valuable information about the neuronal cell loss in the postictal phase. PWI proved to be a sensitive technique for the early identification of regional seizure-induced blood flow alterations with subsequent corresponding decrease in neuronal attenuation.

In this study, the rat pilocarpine model of epilepsy was used. The systemic administration of the cholinergic muscarinic antagonist is a widely used experimental model of SE (16–18, 27). The pilocarpine seizure model is used to study temporal lobe epilepsy, because anatomic changes closely resemble those seen in human mesial temporal sclerosis. After the initially induced SE, a latent period of 2–3 weeks takes place until spontaneous recurrent focal and secondary generalized seizures as well as synaptic reorganization arise following a latent period after SE (26, 28–30). Although initiation of SE by pilocarpine is due to activation of the cholinergic system, the histopathology, neuronal cell loss, and spontaneous seizure activity are thought to be a result of seizure-induced glutamate release (27).

Among the drawbacks of the pilocarpine model is that pilocarpine, even when used at high doses (320–400 mg/kg i.p.), does not always induce SE. In the present study, injection of 360 mg/kg pilocarpine in 32 animals resulted in 20 animals (62.5%) having con-

TABLE 2: Neuronal cell loss determined by cresyl violet staining in different brain regions at different time points after pilocarpin induced SE

	0.5 hours	2 hours	24 hours	1 week	2 weeks
Parietal cortex	99 ± 9%	101 ± 5%	81 ± 7%*	78 ± 5%*	75 ± 9%*
Temporal cortex	98 ± 6%	93 ± 7%	67 ± 3%*	71 ± 5%*	58 ± 10%*
Piriform cortex	93 ± 7%	90 ± 7%	47 ± 3%*	52 ± 12%*	32 ± 4%*
Thalamus	96 ± 4%	100 ± 9%	62 ± 4%*	61 ± 3%*	44 ± 3%*
Amygdala	97 ± 4%	101 ± 10%	66 ± 3%*	54 ± 6%*	38 ± 5%*
Hippocampus (CA1+2)	103 ± 5%	97 ± 7%	70 ± 4%*	63 ± 10%*	52 ± 18%*
Hippocampus (CA3)	99 ± 3%	103 ± 8%	76 ± 3%*	64 ± 11%*	46 ± 20%*

Note.—Values are number of surviving neurons given as percentage of control animals (100%).

tinuous behavioral seizures lasting for 2–8 hours. Furthermore, the use of such high doses is associated with a mortality rate as high as 70% (28), whereby the duration of SE determines mortality rate (27). Although peripheral cholinergic effects and mortality rate can be reduced by injection of scopolamine before pilocarpine administration (15, 22), the 2 hours mortality rate after onset of seizures in this study was 30%. In addition, two animals died within 2 weeks after onset of seizures, so the overall mortality rate in this study was 40%.

Pretreatment of rats with lithium, which markedly potentiates the convulsant action of systemic colinergic agents, allows the dose of pilocarpine to be decreased with subsequent lower mortality and a higher percentage of animals exhibiting SE (31). Despite this advantage, the average latency to the first spontaneous seizures after the application of lithium plus (repeated) low-dose pilocarpine treatment is approximately 40 days (32), which makes this model unsuitable for MR-monitoring perfusion alterations in the very early phase of SE.

Thus, the high-dose pilocarpine model was used in the present study because (1) the chemoconvulsant is easy to administer within the MR scanner, (2) seizures start approximately 10–40 minutes after pilocarpine application and thus, MR-monitoring of the acute phase of SE is possible, (3) when animals have prolonged seizures consistent neuronal damage is observed, (4) previous work has provided a suitable basis for undertaking the current study, and (5) a large percentage of animals exhibit development of temporal lobe epilepsy within a few weeks after the original SE event.

Warach et al (11) were the first do demonstrate that regional hyperperfusion during focal SE can be identified by using functional perfusion-weighted MR techniques: relative cerebral blood volume (rCBV) in the right temporoparietal cortex in a patient in focal SE after a partial resection of a meduloblastoma was 91% higher compared with the contralateral hemisphere. Concordant with this finding, Flacke et al demonstrated an increase in rCBV of 28% in the temporoparietal cortex at 3 hours after onset of nonconvulsive SE in a 68-year old man (12). Recently, Calistri et al described transitory cortical hyperperfusion at 2 days after the onset of epilepsia partialis continua in a 83-year-old woman; relative cerebral blood flow was approximately 35% higher compared with contralateral areas and subsequently decreased to near-normal perfusion at 7 and 15 days after the onset of seizures (10).

As these case reports focused on unilateral SE, MR-derived perfusion of brain parenchyma was normalized relative to the corresponding regions in the contralateral hemisphere. In contrast, the experimental animal model used in this study results in generalized SE and subsequently leads to early neuronal damage and edema formation in both hemispheres as identified with diffusion-weighted MR imaging and histology (24).

To overcome the resulting problem of perfusion normalization, MR-derived brain perfusion was normalized to corresponding regions at baseline conditions, ie, before pilocarpine injection. In saline-treated controls, there was no significant change in relative blood flow indices in all examined regions compared with baseline, confirming that no changes had occurred because of animal handling and injections. We measured the BPR in the bolus-tracking curves as a semiquantitative measure of cerebral perfusion, because this MR technique has been shown to detect subtle perfusion alterations in small regions of interest very accurately (33).

It must be emphasized that absolute cerebral blood flow cannot be computed with this technique, because it depends on the topology of the brain vasculature, which is not known (34). Relative differences in flow between comparable regions, however, can be estimated accurately.

To the best of our knowledge, this is the first experimental MR study by using PWI to detect blood flow alterations at acute time points of less than 3 hours after pilocarpine-induced SE and comparing these changes with the resulting neuronal damage.

Two previous experimental studies examined the subacute phase of seizure-induced damage after kainic acid injection (35, 36) by using DWI. In addition, Wall et al (24) used DWI to detect regional neuronal damage between three and 24 hours after the onset of pilocarpine induced seizures. In this study, histologic verification of neuronal damage was also performed. In all studies, the apparent diffusion coefficient (ADC) reflecting the Brownian motion of water molecules decreased significantly in the retrosplenial and piriform cortex, and the amygdala. Although ADC in the hippocampus also decreased significantly after kainic acid application, there was a rise of 19% in ADC in the hippocampus at 24 hours after onset of pilocarpine-induced seizures, which in-

dicates quantitative differences in the degree of neuronal cell loss within the hippocampus in both models of SE (24)

Currently, there is a debate over mechanisms that may contribute to shifts in ADC after tissue damage resulting from seizures. In animal models of focal brain ischemia, a decrease in ADC is thought to be due to a rapid shift of water from the extracellular to the intracellular compartment (37). The redistribution of intracellular and extracellular water, presumably due to alteration in cell membrane permeability and/or cytotoxic edema, has also been claimed to occur in the acute phase of SE (5, 24, 36)

On the basis of the results of this study, comparable to brain ischemia, a significant local hypoperfusion early after the onset of SE may contributes to decreases in ADC. Local hypoperfusion of the amygdala (62%) and the thalamus (72%) at 0.5–1 hour after the onset of seizures were in the same range as in brain ischemia (61%–63%; measured with PWI in the rat suture model of focal cerebral ischemia), whereas cortical hypoperfusion after the onset of seizures (61%–76%) was less pronounced compared with brain ischemia (35%–39%) (33).

It is interesting that, immediately after the onset of seizures, local blood flow was significantly increased for a couple of minutes in all examined brain regions except the thalamus. This result may be explained by an early increased metabolic rate for oxygen and glucose closely coupled to a measurable increase in blood flow (38). It may be hypothesized that the following decrease in local blood flow as described in this study is due to an early subsequent breakdown of the cell energy state. Thus, a decline of retrosplenial cortical blood flow below 55% (ie, on the level of brain ischemia) seems to be a prognostic threshold value associated with subsequent death of the animal. Concordant with this finding, Dijkhuizen et al (39) showed that relative blood flow indices in brain ischemia could result in irreversible tissue damage.

Neuronal cell loss after pilocarpin-induced SE has been observed in many (40, 41) and partially quantified in some studies (20, 42,). The present study, however, not only gives an extensive analysis of the degree and time course of neuronal cell loss after pilocarpin-induced SE, but also, for the first time, provides evidence for a correlation between changes of CBF in the acute phase of SE and delayed neuronal damage. Therefore, the local decrease in CBF in combination with an SE induced increased metabolic rate in the affected brain regions could be, at least in part, directly responsible for regional neuronal cell loss in the subacute and chronic phase of SE. This hypothesis is also supported by studies on cerebral ischemia, which show delayed neuronal cell death in selected brain regions (especially in the CA1 hippocampus) after short decreases in CBF. As a restriction of this study, brain metabolism and apoptosis after the onset of seizures were not measured. Therefore, this study cannot distinguish between reduced brain perfusion as cause of cell death or whether the reduced brain perfusion only reflects the diminished metabolic demand of dying neurons already committed to apoptosis or necrosis.

The degree of neuronal cell loss observed in this study between 0.5 hours and 2 weeks after SE induction is in line with other studies by using the same model of SE (20, 42). Moreover, several other studies also identified the piriform cortex, the amygdala, and the hippocampus as the brain regions most severely affected by pilocarpin-induced SE (40, 42). Like in the present work, these studies detected the highest degree of neuronal cell loss in these particular brain regions.

Clinical Implications

MR imaging is the diagnostic technique of choice for noninvasive detection of brain abnormalities in SE patients. Seizure-induced chronic brain lesions are visible on T1- and T2-weighted MR images, whereas gross remodeling is detectable by use of hippocampal volumetry (3).

In the very acute phase of SE, T1- and T2-based imaging is limited compared with PWI, because these techniques can only provide information about chronic brain changes. PWI can make available additional physiologic information about ongoing cerebral blood flow alterations associated with acute seizures. In recent years, this technique has been used clinically in the diagnosis and evaluation of ischemic brain disease—namely, stroke (13). Although imaging a patient during a seizure is rare and typically impractible, cerebral blood flow measured by this MR technique gives early valuable information about the extent of neuronal cell loss in the postictal phase.

Conclusion

The key finding of the present study is that PWI is capable of measuring local blood-flow alterations in the acute phase of pilocarpine-induced SE in the rat. Immediately after onset of seizures, PWI demonstrates a transient cerebral hyperperfusion, followed by a significant continuous decline to different perfusion levels. In our experimental setting, a decline of cortical blood flow below 55% of baseline seems to be a prognostic threshold value associated with subsequent death. It is important to note that there is good correlation between the maximal decrease in cerebral blood flow in the acute phase of seizures and late neuronal cell loss. Thus, we have found PWI to be a sensitive MR technique for providing early information about the expected neuronal injury after seizures.

References

1. Treimann DM, Meyers PD, Walton NY, et al. **A comparison of four treatments for generalized convulsive status epilepticus.** *N Engl J Med* 1998;339:792–798
2. Lansberg MG, O'Brian MW, Norbash AM, et al. **MRI abnormalities associated with partial status epilepticus.** *Neurology* 1999;52: 1021–1027
3. Jack CR, Sharbrough FW, Twomey CK. **Temporal lobe seizures: lateralization with MR volume measurements of the hippocampal formation.** *Radiology* 1990;175:423–429

4. Jackson GD, Berkovic SF, Duncan JS, Conelley A. **Optimizing the diagnosis of hippocampal sclerosis using MR imaging.** *AJNR Am J Neuroradiol* 1993;14:753–762
5. Men S, Lee DH, Barron JR, Munoz DG. **Selective neuronal necrosis associated with status epilepticus: Mr findings.** *AJNR Am J Neuroradiol* 2000;21:1837–1840
6. Engel J, Kuhl DE, Phelps ME, Mazziotta JC. **Interictal cerebral glucose metabolism in partial epilepsy and its relation to EEG changes.** *Ann Neurol* 1982;12:510–517
7. Theodore WH, Katz D, Kufta C. **Pathology of temporal lobe foci: correlation with CT, MRI, and PET.** *Neurology* 1990;40:797–803
8. Magistretti P, Uren P, Blume H, et al. **Delineation of epileptic focus by single photon emission tomography.** *Eur J Nucl Med* 1982;7:484–485
9. Marks DA, Katz A, Hoffer P, Spencer SS. **Localization of extratemporal epileptic foci during ictal single photon emission computed tomography.** *Ann Neurol* 1992;31:250–255
10. Calistri V, Caramia F, Bianco F, et al. **Visualization of envolving status epilepticus with diffusion and perfusion MR imaging.** *AJNR Am J Neuroradiol* 2003;24:671–673
11. Warach S, Levin JM, Schomer DL, et al. **Hyperperfusion of ictal focus demonstrated by MR perfusion imaging.** *Am J Neuroradiol* 1994;15:965–968
12. Flacke S, Wuellner U, Keller E, et al. **Reversible changes in echo planar perfusion- and diffusion-weighted MRI in status epilepticus.** *Neuroradiology* 2000;42:92–95
13. Warach S, Li W, Ronthal M, Edelman RR. **Acute cerebral ischemia: evaluation with dynamic contrast enhanced MR imaging and MR angiography.** *Radiology* 1992;182:41–47
14. Mueller TB, Haraldseth O, Jones RA, et al. **Perfusion and diffusion-weighted MR imaging for in vivo evaluation of treatment with U74389G in a rat stroke model.** *Stroke* 1995;26:1453–1458
15. Turski WA, Cavalheiro EA, Schwartz M, et al. **Limbic seizures produced by pilocarpine in rats: behavioural electroencephalographic and neuropathological study.** *Behav Brain Res* 1983;9:315–335
16. Cavalheiro EA, Leite JP, Bortolotto ZA, et al. **Long-term effects of pilocarpine in rats: structural damage of the brain triggers kindling and spontaneous recurrent seizures.** *Epilepsia* 1991;32:778–782
17. Liu Z, Nagao T, Desjardins GC, et al. **Quantitative evaluation of neuronal loss in the dorsal hippocampus in rats with long-term pilocarpine seizures.** *Epilepsy Res* 1994;17:237–247
18. Fujikawa DG. **The temporal evolution of neuronal damage from pilocarpine-induced status epilepticus.** *Brain Res* 1996;725:11–22
19. Turski L, Cavalheiro EA, Turski WA, Meldrum BS. **Excitatory neurotransmission within substantia nigra pars reticulata regulates threshold for seizures produced by pilocarpine in rats: effects of intranigral 2-amino-7-phosphonoheptanoate and N-methyl-D-aspartate.** *Neuroscience* 1986;18:61–77
20. Obenaus A, Esclapez M, Houser CR. **Loss of glutamate decarboxylase mRNA-containing neurons in the rat of the dentate gyrus following pilocarpine-induced seizures.** *J Neurosci* 1993;13:4470–4485
21. Cavalheiro EA, Silva DF, Turski WA, et al. **The susceptibility of rats to pilocarpine-induced seizures is age-dependent.** *Dev Brain Res* 1987;37:43–58
22. Baez LA, Eskridge NK, Schein R. **Postnatal development of dopaminergic and cholinergic catalepsy in the rat.** *Eur J Pharmacol* 1976;36:155–162
23. Villringer A, Rosen BR, Belliveau JW, et al. **Dynamic imaging with lanthanide chelates in normal brain: contrast due to magnetic susceptibility effects.** *Magn Reson Med* 1988;6:164–174
24. Wall CJ, Kendall EJ, Obenaus A. **Rapid alterations in diffusion-weighted images with anatomic correlates in a rodent model of status epilepticus.** *AJNR Am J Neuroradiol* 2000;21:1841–1852
25. Pacinos G, Watson C. *The rat brain in stereotaxic coordinates.* Vol 4. Toronto: Academic Press;1998
26. Minematsu K, Li L, Fisher M, et al. **Diffusion-weighted magnetic resonance imaging: rapid and quantitative detection of focal brain ischemia.** *Neurology* 1992;42:235–240
27. Goodman JH. **Experimental models of status epilepticus.** In: Peterson SL, Albertson TE, eds. *Neuropharmacology methods in epilepsie research.* Boca Raton, FL: CRC Press;1998:95–125
28. Turski L, Ikonomidou C, Turski WA, et al. **Review: cholonergic mechanisms and epileptogenesis: the seizures induced by pilocarpine: a novel model of intractable epilepsy.** *Synapse* 1989;3:154–171
29. Obenaus A, Houser CR. **Neuronal degeneration in the pilocarpine model of chronic seizures: differential vulnerability and time course.** *Epilepsia* 1992;33:36–43
30. Dudek FE, Obenaus A, Schweitzer JS, Wuarin JP. **Functional significance of hippocampal plasticity in epileptic brain: electrophysiological changes in the dentate granule cells associated with mossy fiber sprouting.** *Hippocampus* 1994;4:259–265
31. Honchar MP, Olney JW, Sherman WR. **Systemic cholinerg agents induce seizures and brain damage in lithium-treated rats.** *Science* 1983;220:323–325
32. Glien M, Brandt C, Potschka H, et al. **Repeated low-dose treatment of rats with pilocarpine: low mortality but high proportion of rats developing epilepsy.** *Epilepsy Res* 2001;46:111–119
33. Engelhorn T, Doerfler A, Kastrup A, et al. **Decompressive craniectomy, reperfusion, or a combination for early treatment of acute "malignant" cerebral hemispheric stroke in rats? Potential mechanisms studied by MRI.** *Stroke* 1999;30:1456–1463
34. Weisskoff RM, Chesler D, Boxerman JL, Rosen BR. **Pitfalls in MR measurement of tissue blood flow with intravascular tracers: which mean transit time?** *Magn Reson Med* 1993;29:553–558
35. Wang Y, Majors A, Jajm I, et al. **Posticta alteration of sodium content and apparent diffusion coefficient in epileptic rat brain induced by kainic acid.** *Epilepsie* 1996;37:1000–1006
36. Nakasu Y, Nakasu S, Morikawa S, et al. **Diffusion-weighted MR in experimental sustained seizures elicited with kainic acid.** *AJNR Am J Neuroradiol* 1995;16:1185–1192
37. Sotak CH. **Nuclear magnetic resonance (NMR) measurement of the apparent diffusion coefficient (ADC) of tissue water and its relationship to cell volume changes in pathological states.** *Neurochem Int* 2004;45:569–582
38. Duncan R, Patterson J, Roberts R. **Ictal regional cerebral blood flow in frontal lobe seizures.** *Seizure* 1997;6:393–401
39. Dijkhuizen RM, Berkelbach van der Sprenkel JW, Tulleken KA, Nicolay K. **Regional assessment of tissue oxygenation and the temporal evolution of hemodynamic parameters and water diffusion during acute focal ischemia in rat brain.** *Brain Res* 1997;750:161–170
40. Roch C, Leroy C, Nehlig A, Namer IJ. **Magnetic resonance imaging in the study of the lithium-pilocarpine model of temporal lobe epilepsy in adult rats.** *Epilepsia* 2002;43:325–335
41. Zhang X, Cui SS, Wallace AE, et al. **Relations between brain pathology and temporal lobe epilepsy.** *J Neurosci* 2002;22:6052–6061
42. Peredery O, Persinger MA, Parker G, Mastrosov L. **Temporal changes in neuronal dropout following inductions of lithium/pilocarpine seizures in the rat.** *Brain Res* 2000;881:9–17